

# **The Role of Potential Energy Surface in Quantum Mechanical Tunneling: A Computational Perspective**

**Thesis submitted to the  
Thapar Institute of Engineering & Technology**



**THAPAR INSTITUTE  
OF ENGINEERING & TECHNOLOGY  
(Deemed to be University)**

**For the degree of  
MASTER OF SCIENCE  
IN CHEMISTRY**

**Submitted By**

**REENA**

**(301702023)**

**Under the supervision of**

**Dr. DEBASISH MANDAL**

**ASSISTANT PROFESSOR**

**SCHOOL OF CHEMISTRY AND BIOCHEMISTRY  
THAPAR INSTITUTE OF ENGINEERING & TECHNOLOGY  
PATIALA-147004 (India)**

**August 2019**

## SELF DECLARATION

The work embodied in the project entitled "**The Role of Potential Energy Surface in Quantum Mechanical Tunneling: A Computational Perspective**" has been done by me in the partial fulfillment of requirement for the award of degree of **Master of Science in Chemistry**, submitted in the **School of Chemistry and Biochemistry, Thapar Institute of Engineering and Technology, Patiala**, is an authentic record of my own carried out under the supervision and guidance of **Dr. Debasish Mandal**, Assistant Professor of School of Chemistry and Biochemistry TIET, Patiala. All the ideas and references have been duly acknowledged.

Reena

Reena

Date: 12/08/2019

This is to certify the above statement made by student concerned is correct and true to the best of my knowledge.

Dr. Debasish Mandal  
12/08/2019

Dr. Debasish Mandal

Assistant Professor

School of Chemistry and Bio-chemistry

Thapar Institute of Engineering and Technology, Patiala

## CERTIFICATE

This is to certify that the thesis entitled "The Role of Potential Energy Surface in Quantum Mechanical Tunneling: A Computational Perspective" being submitted by Reena, to the School of Chemistry and Biochemistry, Thapar Institute of Engineering and Technology, Patiala for the award of degree of Masters of Science, is a record of bonafide research work carried out by her. Miss Reena has worked under my guidance and supervision and has fulfilled the requirements for submission of thesis, which to my knowledge has reached the requisite standard.

The results embodied in the thesis have not been submitted in part or full to any other University or Institute for the award of any degree or diploma.

*Dmandal*  
*12/08/19*

Dr. Debasish Mandal

Assistant Professor

School of Chemistry and Bio-chemistry

Thapar Institute of Engineering and Technology, Patiala

# **TABLE OF CONTENT**

<b>Acknowledgements</b>	<b>v</b>
<b>Abstract</b>	<b>vi</b>
<b>Acronyms and Abbreviations</b>	<b>vii</b>
<b>List of Tables</b>	<b>viii</b>
<b>List of Figures</b>	<b>viii</b>
<b>1. Introduction</b>	<b>1</b>
<b>2. Theoretical Background and Detailed Computational Methodology</b>	<b>4</b>
2.1 Schrodinger Equation Underpinned Theoretical Chemistry	4
2.2 Born-Oppenheimer Approximation	5
2.3 Hartee-Fock Self Consistent Field Method	6
2.4 Density Functional Theory	7
2.5 Functionals	8
2.6 Basis Set	8
2.7 Complete Basis Set	9
2.8 Potential Energy Surface	10
2.9 Computational Methodology	11
<b>3. Results and Discussion</b>	<b>12-19</b>
<b>4. Conclusion</b>	<b>20</b>
<b>5. References</b>	<b>21-23</b>

## **ACKNOWLEDGEMENT**

With deep regards and profound respect, I avail this opportunity to express my deep sense of gratitude and indebtedness to my supervisor, **Dr. Debasish Mandal**, School of Chemistry and Biochemistry, Thapar Institute of Engineering & Technology for introducing the present thesis topic and for his inspiring guidance, constructive criticism and valuable suggestion throughout the work. I most gratefully acknowledge his constant encouragement and help in different ways to complete this thesis successfully.

I acknowledge my sincere regards to the **Head** and all staff's member of **School of Chemistry & Biochemistry, Thapar Institute of Engineering & Technology** for their kindness and support. We are also thankful to SCBC, T.I.E.T and INSPIRE FACULTY GRANT [DST/INSPIRE/04/2016/001948] for providing computational facilities.

Further I am highly obliged to all my friends for their consistent encouragement and succor. Words are not enough to express my feelings about my immense gratitude that I owe to my dear Parents for their endless love, blessings and moral support throughout my life. Last but not the least I am thankful to all the persons who helped me directly or indirectly during the tenure of my project work.

Place: PATIALA

Date:

**REENA**

## **ABSTRACT**

The work presented here seeks to intensify our understanding of quantum mechanical tunneling (QMT) in hydrogen atom transfer (HAT) reactions. The work focuses on two sorts of the reactions: (i) HAT from different substrate by same radical abstractor and (ii) HAT from same substrate by different radical abstractor. We corroborate QMT in the chemical reactions with an efficient exploration of potential energy surface (PES) using computational approach. The PESs are computed using composite CBS-QB3 method and the obtained energetics are utilized to determine the rate constant for these aforementioned reactions. The rate constants including the effect of tunneling through the barrier have been calculated at three different temperatures 77K, 273K and at 298K. Tunneling corrected KIE values have also been computed using semi-classical Eyring's transition state theory equation and compared with the available experimental findings to ascertain the reliability of the tunneling contribution. It is observed that the probability of tunneling is highly dependent on the symmetry & the narrowness of the PESs. Thereby, this work gives an insight into the importance of tunneling and its contributing factors in simple H-atom transfer reactions.

**Key Words:** Potential Energy Surface, Quantum Mechanical Tunneling, Reaction rate, Hydrogen atom transfer reactions, Kinetic Isotope Effect.

## **ACRONYMS AND ABBREVIATIONS**

APNO	Atomic Pair Natural Orbital
CBS	Complete Basis Set
CC	Coupled Cluster
CI	Configuration Interaction
CGTO	Contracted Gaussian type orbitals
DFT	Density Functional Theory
ECP	Effective Core Potential
GGA	Generalised Gradient Approximation
GTO	Gaussian Type Orbitals
HAT	Hydrogen Abstraction Reaction
HF	Hartee-Fock Theory
HK	Hohenberg-Kohn Theorem
IF	Imaginary Frequency
IRC	Intrinsic Reaction Coordinates
KIE	Kinetic Isotopic Effect
KS	Kohn-Sham Theorem
LCAO	Linear Combination of Atomic Orbitals
LDA	Local Density Approximation
MO	Molecular Orbitals
PES	Potential Energy Surface
PGF	primitive Gaussian function
QMT	Quantum Mechanical Tunneling
SCF	Self Consistent Field
STO	Slater's Type Orbitals
TS	Transition State
TST	Transition State Theory
ZPE	Zero-Point Energy

## LIST OF TABLES

<b>Table 3.1.</b>	Rate constants $k$ ( $\text{cm}^3 \text{ molecule}^{-1} \text{ s}^{-1}$ ), quantum corrections $k$ , kinetic isotope effect ( $k_{\text{H}}/k_{\text{D}}$ ) for the H-abstraction reactions at 77K	15
<b>Table 3.2.</b>	Rate constants $k$ ( $\text{cm}^3 \text{ molecule}^{-1} \text{ s}^{-1}$ ), quantum corrections $k$ , kinetic isotope effect ( $k_{\text{H}}/k_{\text{D}}$ ) for the H-abstraction reactions at 273K	15
<b>Table 3.3.</b>	Rate constants $k$ ( $\text{cm}^3 \text{ molecule}^{-1} \text{ s}^{-1}$ ), quantum corrections $k$ , kinetic isotope effect ( $k_{\text{H}}/k_{\text{D}}$ ) for the H-abstraction reactions at 298K	16
<b>Table 3.4.</b>	Tunneling efficiency (% tun) calculated for the reactions of scheme 1.1 & scheme 1.2 at $T = 273\text{K}$ and $298\text{K}$	17

## LIST OF FIGURES

<b>Figure 3.1.</b>	Optimized geometries with geometrical parameters of stationary points and qualitative representation of the potential energy profile of the reaction scheme 1.1 using CBS-QB3 theoretical method.	12
<b>Figure 3.2.</b>	Optimized geometries with geometrical parameters of stationary points and qualitative representation of the potential energy profile of the reaction scheme 1.2 using CBS-QB3 theoretical method.	14
<b>Figure 3.3.</b>	Potential Energy ( $E$ , kcal/mol) vs Intrinsic Reaction Coordinates ( $\text{amu}^{1/2} \text{ bohr}$ ) for H-abstraction reaction from scheme 1.2 by TS3 and TS4 computed at B3LYP/CBSB7 level of theory.	19

# Chapter 1

---

## Introduction

One of the greatest challenges in chemistry is to understand how chemical reaction proceeds. While studying the chemical reaction, one is generally anxious about knowing the reaction mechanism with the followed trajectory and the rate at which it proceeds i.e., the subject of chemical kinetics. An efficient exploration to chemical reaction is the study of transition state theory (TST) which established the concept of potential energy surface (PES). Information on kinetics formulated by Eyring's TST<sup>1</sup> Eq.1.1 of rate constant and mechanistic aspects by PES study provides essential connections between molecular structure and reactivity.

$$k = \kappa (k_B T/h) e^{-\frac{\Delta G^\ddagger}{RT}} \quad \text{---Eq.1.1}$$

where  $\Delta G^\ddagger$  is the relative Gibbs free energy of the transition state with reactants,  $k_B$  is the Boltzmann's constant,  $h$  is the planck's constant and  $\kappa$  is the transmission coefficient that incorporated the tunneling corrections. Chemical reaction may pursue multiple pathways, either classical (over the barrier) pathway or quantum (through the barrier) pathway<sup>4</sup> implies via tunneling, resulting in the understanding of chemical reactions. Investigations of the chemical transformations possesses quantum characteristic emphasizes the need and importance of theoretical studies.

Most interesting and at the same time epidemic quantum mechanical phenomenon is tunneling with a dominant contribution to the rates of many chemical reactions. Tunneling is the quantum effect which allows the particles (having wave-like nature) to penetrate through the potential energy barrier although lacking of energy to conquer them. Tunneling particles prefers to travels across the higher potential energy region at the expense of reduced barrier width. Being sensitive to barrier height and width, tunneling is admissible when the de Broglie wavelength of the particle is of the same order of barrier width. Meanwhile the energetic effect of tunneling lowers the semi-classical barrier and helps the chemical transformation. We expanded our studies, thus the obvious manifestation of probability of tunneling is dependent on mass of the particle  $m$ , height of the barrier  $E_a$ , and the width of the barrier. These are the dominant parameters controlling the tunneling reaction rate.<sup>2-3</sup> Thus, tunneling is mostly restricted to-lighter (mass) atoms, and has advanced our understanding towards the various (bio)chemical reactions involving electrons, proton, hydrogen or hydride atom transfers.<sup>3</sup> But with the time, tunneling was also investigated for heavy atoms. It is

impossible to mention all the investigations that have been performed till now to establish the importance of tunneling in chemical & biological reaction. We can only mention a few them.

**Electron tunneling:** *Winkler and Gray* investigated the electron tunnel amongst the various sites in biological redox chains to facilitate biological reactions.<sup>4</sup>

**Hydrogen or hydride tunneling:** *Truhlar* shared viewpoint on the proton tunneling in various ensemble enzymatic and non-enzymatic reactions.<sup>5</sup> In addition, *Klinman* probed the role of hydrogen tunneling in enzyme systems specifically encountering the alcohol dehydrogenase reactions.<sup>6</sup> *Breslow and his co-workers* evidently discovered that quantum mechanical tunneling plays significant role in hydride transfer mechanism for isomerisation of glyceraldehyde in prebiotic reactions.<sup>7</sup> *Schreiner and his co-workers* shows the unexceptional reactivity of o-nitrobenzaldehyde in the photorearrangement reaction. As the mimicking behavior of many carboxylic compounds led to the formation of product via H-tunneling.<sup>8</sup> He also premeditated conformational changes in carboxylic acids, especially various biological molecules undergoes rotamerization which is attributed by H-tunneling.<sup>9</sup>

**Carbon tunneling:** *Sheridan et. al.* reviewed the carbenic rearrangement reaction which featured the carbon tunneling in the ring expansion of noradamantylchlorocarbene.<sup>10a</sup> Similarly, *Schreiner and his co-workers* studied that carbon tunneling contributes significantly to yield cyclobutene as product in the ring expansion of the parent compound i.e. cyclopropylcarbene.<sup>10b</sup>

Tunneling also found very much important in C-H activation catalyzed by high-valent Fe(IV)O complexes.<sup>12-14</sup>

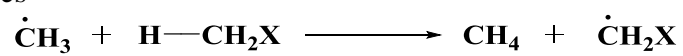
Thus, it has been noted that the quantum effects like tunneling, most prominently can occur in various areas of science.<sup>11</sup> Currently, Hydrogen atom transfer (HAT), ubiquitous in majority of (bio)chemical reactions, has garnered the significant attention in theoretical studies because of the possibility of the presence of tunneling.

Considering above, our goal is to study the simple representative (hydrogen atom transfer/abstraction reaction) reaction with an efficient exploration of potential energy surface (PES) of the reaction using the quantum computational approach. We basically studied two types of reaction with the aim of understanding the reactivity pattern and the role of tunneling e.g.

(i) HAT from different substrate by same radical abstractor presented in scheme 1.1.

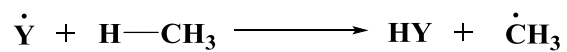
(ii) HAT from same substrate by different radical abstractor given in scheme 1.2.

**Scheme 1.1.** General Reaction Scheme for methyl radical abstracting hydrogen atom from different substrates



where X= H, NH<sub>2</sub>, OH

**Scheme 1.2.** General Reaction Scheme for different radical abstracting hydrogen atom from methane



where Y= OH, OOH, OCH<sub>3</sub>, CH<sub>3</sub>

## Chapter 2

---

### Theoretical Background and Detailed Computational Methodology

Chemistry is one of the novel science disciplines, generally concerned with the chemical transformations through ‘breaking’ and ‘forming’ of bonds and the central fundamental things is to realize every step of it i.e., called reaction mechanism. Exploration of the reaction mechanism is quite difficult even at the state-of-art technique due to the presence of short lived intermediate, multiple reaction pathways etc. Computational chemistry can be a complementary tool of the experiment in this aspect.

Computational chemistry is a technique used to solve chemical problems using suitable computer programming/algorithm. Schrodinger equation can't be exactly solved for multi-electron system even after using advanced mathematics or powerful computer.<sup>15</sup> So, the central task is to understand the nature of the chemical system for the given n-electron system by solving the Schrodinger equation approximately to obtain the wave function which depicts the physical properties and total energy of the system. In the following sections, we are going to preface some of the basic principles of quantum chemistry followed by computational techniques that allow us to find the quantitative solution to distinct problems of electronic structure theory.<sup>16</sup> Computational chemistry is the modernist approach to various complexes, stagnant and pragmatic models of chemical systems. It not only solves the equations of quantum mechanics but also the equations of classical mechanics with relative ease.

#### **2.1 Schrodinger Equation Underpinned Theoretical Chemistry**

To describe a physical system in quantum mechanics a function is introduced called the “wave function” denoted by Greek letter  $\Psi$ . It is a function of electronic and nuclear coordinates containing the complete information about the system and gives away an observable property of the system when an appropriate operator *e.g.*, “Hamiltonian” is applied to it, which describes the total energy of the system, leading to the following Schrodinger's equation:

$$\hat{H}\Psi = E\Psi \quad \text{-- Eq. 2.1}$$

where  $\hat{H}$  is the Hamiltonian operator,  $\Psi$  is the wavefunction (eigenfunction for a given Hamiltonian) and  $E$  is the energy of the system and the time-dependent Schrodinger's equation is given by:

$$i\hbar \frac{\partial}{\partial t} \Psi(\mathbf{q}, t) = -\frac{\hbar^2}{2m} \frac{\partial^2 \Psi(\mathbf{q}, t)}{\partial q^2} + V(\mathbf{q}, t) \Psi(\mathbf{q}, t) \quad \text{--Eq.2.2}$$

where the wavefunction  $\Psi$  depends upon the spatial coordinates ( $\mathbf{q}$ ) of electrons and nuclei of the system and the time ( $t$ ).

In general,  $\hat{H}$  can be expanded as:

$$\hat{H} = T_e + T_n + V_{ne} + V_{ee} + V_{nn} \quad \text{--Eq.2.3}$$

where  $T_e$  and  $T_n$  are the kinetic energy operators for electrons and nuclei respectively,  $V_{ne}$  represents attractive potential energy between electrons and nuclei,  $V_{ee}$  and  $V_{nn}$  represents inter-electronic and inter-nuclear repulsion potential energy respectively. Different terms involved in the above Eq.2.3 are written as:

$$\begin{aligned} \hat{T}_e &= -\frac{1}{2} \sum_{i=1}^N \nabla_i^2 \quad ; \quad \hat{T}_n = -\frac{1}{2} \sum_{A=1}^M \frac{1}{M_A} \nabla_A^2 \\ \hat{V}_{ne} &= -\sum_{i=1}^N \sum_{A=1}^M \frac{Z_A}{r_{iA}} \\ \hat{V}_{ee} &= \sum_{i=1}^N \sum_{j>i}^N \frac{1}{r_{ij}} \quad ; \quad \hat{V}_{nn} = \sum_{A=1}^M \sum_{B>A}^M \frac{Z_A Z_B}{R_{AB}} \end{aligned} \quad \text{--Eq.2.4}$$

Now  $H$  can be written as:

$$H = -\frac{1}{2} \sum_{i=1}^N \nabla_i^2 - \frac{1}{2} \sum_{A=1}^M \frac{1}{M_A} \nabla_A^2 - \sum_{i=1}^N \sum_{A=1}^M \frac{Z_A}{r_{iA}} + \sum_{i=1}^N \sum_{j>i}^N \frac{1}{r_{ij}} + \sum_{A=1}^M \sum_{B>A}^M \frac{Z_A Z_B}{R_{AB}} \quad \text{--Eq.2.5}$$

where A and B denotes the M nuclei and i, j denotes the N electrons system.

There are several approximations were taken in computational quantum chemistry to solve Schrodinger equation for multi-electron system. Few of them are discussed as follows:

## **2.2 Born- Oppenheimer Approximation**

Referring to previous argument,  $\Psi$  is the function of the position of electrons and nuclei of the system. Due to large mass difference between nuclei and electrons, Born-Oppenheimer approximation declares that electrons move faster than nuclei and the motion of nuclei is considered to be frozen whereas neglecting all other relativistic effects. To this, it presumes that the kinetic energy of nuclei to be zero yet partly responsible for the potential energy of

the system. Applying this approximation to Eq.2.5 second term is no longer necessary and the final term, nuclear repulsion is omitted (constant term doesn't bother to wave function). Now, the Schrodinger's equation involving the purely electronic Hamiltonian is written as:

$$\hat{H}_{\text{elec}}\Psi_{\text{elec}} = E_{\text{elec}}\Psi_{\text{elec}} \quad \text{--Eq.2.6}$$

Potential energy surface concept is the after-effect of this approximation. It is well known that Born-Oppenheimer approximation is not globally bonafide for exact solution of electronic Schrodinger equation for n-electron systems as the inter-electronic repulsion term makes it impossible.<sup>16</sup>

### **2.3 Hartree-Fock Self-Consistent Field Method**

With objective to solve many electron system problem, preceding approximation bring ups the subject that inter-electronic repulsion makes Schrodinger equation non separable and not exactly solved. So, laid groundwork (new approximation) for many quantum mechanical problems called Hartree-Fock (HF) approximation, which is also known as Self-Consistent Filed Theory (SCF).<sup>16</sup> With respect to set good approximation to obtain the ground state energy of n-electron system HF addressed that each electron experiences the repulsion in average fashion rather than explicit electron-electron interactions i.e. each electron moves entirely free (irrespective of all others) in an average field led by other electrons. Electrons are enclosed to spin orbitals and changes in order to attain minimal energy which is accomplished via variational principle, thereby producing the Eq.2.7 called HF equation-

$$\mathbf{F}\phi_i = \varepsilon_i \phi_i \quad \text{--Eq.2.7}$$

Where  $\mathbf{F}$  is the Hartree-Fock operator,  $\varepsilon_i$  corresponds to the energy of the  $i^{\text{th}}$  spin-orbital  $\phi_i$ . The Hartree-Fock operator  $\mathbf{F}$  is expressed as the sum of one electron core Hamiltonian and the HF potential, corresponds to coulomb and exchange integrals terms.

Self-Consistent Field (SCF) method describes the electronic interactions in terms of mean-field, the non-existence of antisymmetric nature of wavefunction whereas, HF assumes inter-electronic interaction as an average potential resulting to a single determinant solution, thereby assuming that one determinant is a sufficient description of wavefunction, which includes the antisymmetric nature of the wavefunction.

Two major shortcomings of HF method are that, hypothetically each energy eigenfunction is interpretable by single slater-determinant which doesn't consider the coulomb correlation and secondly the instantaneous interaction between the electrons pairs i.e. neglecting the correlation between electrons with the same spin. Thus, the induced correlation problem in HF energy is defined as the correlation energy.

$$E_{\text{corr}} = E_{\text{tot}} - E_{\text{HF}} \quad \text{--Eq.2.8}$$

where,  $E_{\text{corr}}$  is the missing energy,  $E_{\text{HF}}$  is the Hartree-Fock energy which is always greater than the exact non-relativistic energy  $E_{\text{tot}}$ . Most of the techniques practice the HF approximation as initiation, to correlate electrons by more précised computational methods. Fleshed with new approximation theory, “post-hartree-fock” method which includes the Configuration Interaction (CI), Moller-Plesset Perturbation theory<sup>26</sup> and Coupled Cluster (CC) theories.<sup>27</sup> However, these theories are not exercised in this thesis, so not continued.

## **2.4 Density Functional Theory**

The speculation behind Density Functional Theory (DFT)<sup>17</sup> is that energy of the system is computed from electron density which serves as fundamental quantity rather than the wavefunction. This theory is premised on two theorems namely, Hohenberg-Kohn (HK)<sup>18</sup> theorem and Kohn-Sham (KS) approach.<sup>19</sup> Firstly, Hohnberg-Kohn theorem states that ground state energy is a functional of both the potential and the electron density. Thus, electron density provides a minimum ground state energy using the variational calculus. But HK yields a poor representation of obtaining the ground state energy from the electron density and unable to explain a way of acquiring the electron density. Then Kohn-Sham realised that problem lies with the way kinetic energy is depicted. Therefore, KS devised a method having similar approach as Hartree-Fock (system is described by single determinant wavefunction) by replacing the interacting system with an auxiliary non-interacting system in an effective local potential. In this formulation, the electron density is expressed as a linear combination of basis functions similar to HF orbitals. For exact functional, orbitals (from these functions) need to yield exact ground state density thus, ground state energy and potential, where potential is substituted by the exchange-correlation potential.

$$E = T_{\text{ni}} + V_{\text{ne}} + V_{\text{ee}} + \Delta T + \Delta V_{\text{ee}} \quad \text{--Eq.2.9}$$

Aforesaid that  $E$  is function of electron density, where  $T_{\text{ni}}$  is the kinetic energy of the non-interacting system,  $V_{\text{ne}}$  the attraction between nuclei and electrons,  $V_{\text{ee}}$  is the classical electron-electron repulsion, latter two terms are collectively exchange – correlation energy constituting the correction to kinetic energy and non- classical components of electronic repulsion energy. Exchange-correlation energy is unknown and is advanced with various functional treatments to compute the accurate energy. These functional treatments are not further discussed in details but brief outline is examined in next section. Also, above stated overview of DFT is less detailed but worthy understanding.

## **2.5 Functionals**

To investigate the total energy of the system, further multiple approximations (functionals) were developed to find this the exchange-correlation energy. These functional are mainly described by three exchange-correlation components: (i) Local Density Approximation (LDA)<sup>20</sup> (ii) Generalised Gradient Approximation (GGA)<sup>21</sup> and (iii) Hybrid Functionals. Anyway, generalised gradient functional consists of electron density gradient, usually solving the exchange and correlation terms individually. Hybrid functional formulates exchange functional as the linear combination of HF, local and gradient-corrected exchange terms.

For example, B3LYP<sup>22</sup> is the commonly used hybrid approach for studying exchange correlation and used in our present study as functional. B3 is the exact exchange functional, part of hybrid functional which was developed by Becke whereas LYP is the GGA correlation functional, which was proposed by Lee-Yang-Parr. This combination of exchange and correlation is made to describe the complete system.

## **2.6 Basis Set**

In chemistry, basis set is a set of functions (non-orthogonal) that elucidate the state of the molecular system. These functions correspond to atomic orbitals, basically used to build molecular orbitals (MO). These functions are centered on atoms specifically each atomic nucleus, but there is possibility to have basis functions centered on bonds and are expanded as linear combinations of atomic orbitals with coefficients, which was often referred in the LCAO-MO (linear combination of atomic orbitals) approximation.<sup>16</sup>

Molecular wavefunction comprise of both a radial and spherical components, where illustration of radical part is the key component of the basis functions. Primarily there exists two types of basis functions namely, Slater's Type Orbitals (STO) and Gaussian Type Orbitals (GTO). Although STO's resembles the behavior of hydrogenic orbitals which is quite evident from exponential dependency i.e. distance between the nucleus and the electron. The key difference between both is: the use of normalization factor, spherical coordinates, angular momentum and the exponential dependence ( $e^{-\zeta r}$ ) in STO's whereas, GTO's uses the normalization factor, cartesian coordinates and exponential dependence ( $e^{-\zeta r^2}$ ) for the description of atomic orbitals in their mathematical expression. However, the calculations with Slater orbitals is computationally demanding but the calculations of two or more center two electron integrals became extremely slow. Therefore, the use of GTO's makes computational easy but functionally they lacks a cusp at nucleus. So, consequently STO's are approximated as linear combinations of Gaussian orbitals, as result, obtaining contracted

Gaussian type orbitals (CGTO). Depending upon the molecular system basis sets are further classified along with the functional modification.

- *Minimal Basis Set* is the smallest basis set composed of minimum number of basis functions. For example, STO-3G basis set is the smallest minimal basis set indicating that each basis function uses 3GTO's (primitive Gaussian) to resemble Slater type orbitals.
- *Split-Valance Basis Set* is to depict the valence orbitals (valence electrons taking part in the molecular bonding). These are X-YZg type where X,Y,Z are integers. For example, 6-31G basis set, which illustrate that core orbitals are described by six primitive Gaussian function (PGF) and valence orbitals splitted into two basis function, one is composed of three PGF and other only one.

Moreover, polarized functions are exercised to basis set for the flexibility of the orbital as another atom approaches it.

- *Diffuse Basis Set* uses diffuse function to identify the wavefunction, are indicated as '+' sign. For example, 6-31+G describing the part of atomic orbitals distant from the nuclei. The molecular system containing lone pair, anions or to heavy atom system, also molecular system possessing low ionization potential contributes to the Gaussian basis function and hence, corresponds to atomic orbital shape with more accuracy.
- *Effective Core Potential (ECP)* and many more.

This thesis primarily doesn't contain any application of other basis set.

## **2.7 Complete Basic Set (CBS)**

The composite ab initio CBS method emulates an infinitely large basis set with aim to predict highly accurate molecular energy of system at relatively low computational cost. There are three basic members of CBS methods: CBS-4M,<sup>23</sup> CBS-QB3<sup>24</sup> and CBS-APNO<sup>25</sup> in ascending order of accuracy. The APNO (Atomic Pair Natural Orbital) version being most accurate, still we preferred CBS-QB3 as it is much faster at relatively low computational cost. Essential steps involved in CBS-QB3 method<sup>24</sup>:

- A geometry optimization and frequencies at B3LYP/CBSB7 where, B3LYP functional calculations are performed with 6-311G(2d,d,p) basis set.
- Single point energy calculations are executed at CCSD(T)/6-31+G(d') and MP4SDQ/CBSB4 levels.

- With an extrapolation to infinite basis set limit using natural pair orbitals energy at the MP2/CBSB3 level together with an additive correction at CCSD(T) level, to yield the total energy of the system.

## **2.8 Potential Energy Surface (PES)**

A PES is the graphical representation which aids us visualizing and understanding the molecular geometry corresponding to the potential energy. One of the cornerstones of PESs is its stationary points for examine the chemical reactions. As significance, molecules like to be at lowest possible energy. Thus, stationary points corresponding to actual molecules with measurable lifespan are energy minima points. These necessary points evaluated on a PES are classified corresponding to the first and second derivative of the energy. Mathematically, stationary points are characterized by a null first derivative of the potential energy with respect to each geometric parameter:

$$\frac{\partial V}{\partial q_1} = \frac{\partial V}{\partial q_2} = \dots = 0 \quad \text{--Eq.2.10}$$

So, these energy minima all are positive by curvature whereas saddle point is the maximum connecting two minima's depicted by negative curvature in one direction and positive in all other direction corresponds to the transition state. Distinguishing these minima and maxima, we can write:

At minima, second derivatives are positive due to positive curvature:

$$\frac{\partial^2 V}{\partial q^2} > 0$$

And at saddle point, one of second derivative is negative whereas all other are positives i.e.

$$\frac{\partial^2 V}{\partial q^2} < 0$$

And

$$\frac{\partial^2 V}{\partial q^2} > 0$$

In addition, it is analyzed that force constant ( $k$ ) is given by the second derivative of the potential energy, logically force constant is proportional to the frequency ( $\nu$ ) of the molecule or vice-versa.

$$k = \frac{\partial^2 V}{\partial R^2} \quad \text{and} \quad \nu = \frac{1}{2\pi c} \sqrt{\frac{k}{\mu}} \quad \text{--Eq.2.11}$$

Focusing on the above data, further analysis will be discussed in next section.<sup>15</sup>

## **2.9 Computational Methodology**

All the calculations briefed in this study were carried out with the help of GAUSSIAN 16 program.<sup>28</sup> We carried out the calculations using high-level composite method: CBS-QB3, based on CBS model. For depiction of transition states (one imaginary frequency), zero-point energy (ZPE) correction and the stationary points as minima (no imaginary frequency) etc., vibrational frequencies were studied at B3LYP/CBSB7 theoretical level. Intrinsic reaction coordinate (IRC) calculations assure that the computed transition state structures connect the desired reactant and product, were performed at B3LYP/CBSB7 theoretical level. Using IRC calculations we tried to comprehend the narrowness of the potential energy barrier.

We calculated the reaction rates for all reacting systems using TheRate program<sup>29</sup> and obtained rate constants, also tunneling transmission coefficient using Eckart barrier.<sup>29</sup> H-D Kinetic isotopic effect (KIE) value were calculated using Eyring equation obtaining the required data from the rate output file for all the reactions and compared with the reported experimental data to ascertain the reliability of the tunneling contribution. As experimental data was reported at 77K, we collectively measured the rate data at three different temperatures i.e. 77K for comparison, 273K and 298K for differentiating the rate studies at different temperatures.

Moreover, for producing the inputs and visualization of the molecular structures and for analyzing the computed results we used Chemcraft program.<sup>30</sup>

## Chapter 3

### Results & Discussion

To systematically investigate the nature of H-abstractions the CBS-QB3 PES has been drawn separately for both scheme 1.1 & 1.2. The sum of the energies of the reactants are assumed as zero for reference in the PES. Secondly, we have also calculated the rate constants, transmission coefficients and tunnelling corrected KIE and the results are presented in the tabulated form. The transition state geometries along with key geometrical parameters are also presented in the PESs profile.

#### Description of PES of Scheme 1.1:

The PES related to the reactions of scheme 1.1 and the corresponding transition states are depicted in figure 3.1.

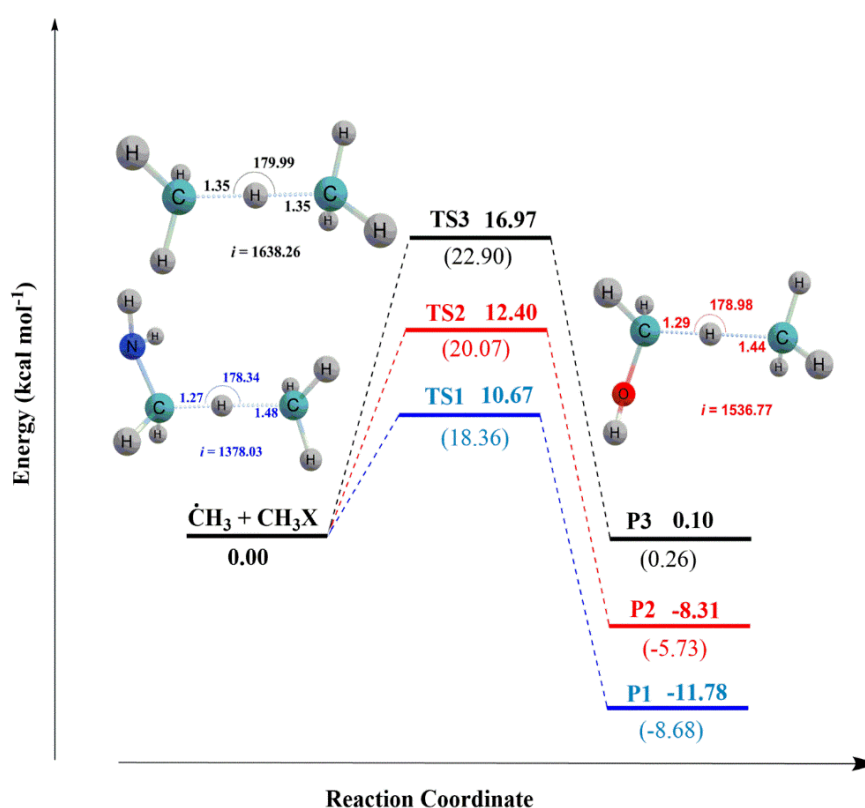


**Figure 3.1.** Optimized geometries with geometrical parameters of stationary points and qualitative representation of the potential energy profile of the reaction scheme 1.1 using CBS-QB3 theoretical method. Note that the relative electronic energy (kcal/mol) with ZP correction outside the parentheses and relative gibbs free energy with ZP correction inside the parentheses.

**Reaction between CH<sub>3</sub> radical & CH<sub>3</sub>NH<sub>2</sub>:** The product P1 is formed via the transition state TS1 where CH<sub>3</sub> radical is abstracting hydrogen from carbon of methylamine which exhibits 10.67 kcal/mol energy of activation. The H-abstraction takes places roughly in linear fashion with angle 178.34° in which H-CH<sub>2</sub>NH<sub>2</sub> distance is 1.27 Å and H-CH<sub>3</sub> distance is 1.48 Å. The TS1 contains an imaginary frequency 1378.03 cm<sup>-1</sup>.

**Reaction between CH<sub>3</sub> radical & CH<sub>3</sub>OH:** The product P2 is formed via the transition state TS2 possesses 12.40 kcal/mol energy of activation where CH<sub>3</sub> radical is abstracting hydrogen from carbon of methanol with bond forming H-CH<sub>3</sub> 1.44 Å distance and H-CH<sub>2</sub>OH distance is 1.29 Å. The TS2 comprises an imaginary frequency 1536.77 cm<sup>-1</sup>.

**Reaction between CH<sub>3</sub> radical & CH<sub>4</sub>:** The product P3 is formed by the direct attack of CH<sub>3</sub> radical on the carbon atom of CH<sub>4</sub> in linear fashion with angle 179.99° via the transition state TS3 with the barrier of 16.97 kcal/mol. The bond breaking H-CH<sub>3</sub> distance is same as the bond making H-CH<sub>3</sub> distance which is 1.35 Å. In this reaction pathway, we observed the symmetry within the PES. The imaginary frequency corresponds to TS3 is 1638.26 cm<sup>-1</sup>.

#### **Description of PES of Scheme 1.2:**

The next is to investigate nature of abstractor via PES profile figure 3.2 for the reactions of scheme 1.2, in which different radicals tends to abstract hydrogen atom from the same substrate i.e. methane.

**Reaction between OH radical & CH<sub>4</sub>:** The product P4 is formed via the transition state TS4 having the lowest energy barrier of 4.15 kcal/mol. The hydrogen atom is abstracted at the angle 170.68° with the O-H distance of 1.29 Å whereas C-H distance is 1.23 Å. The imaginary frequency of TS4 is 1104.86 cm<sup>-1</sup>.

**Reaction between OCH<sub>3</sub> radical & CH<sub>4</sub>:** The product P5 is formed by the direct attack of oxygen atom to abstract the hydrogen from CH<sub>4</sub> via the transition state TS5 possessing second lowest energy barrier of 10.77 kcal/mol and the imaginary harmonic frequency for TS5 is 1664.70 cm<sup>-1</sup>. The abstracting O-H distance is 1.88 Å and the C-H distance is 1.32 Å.

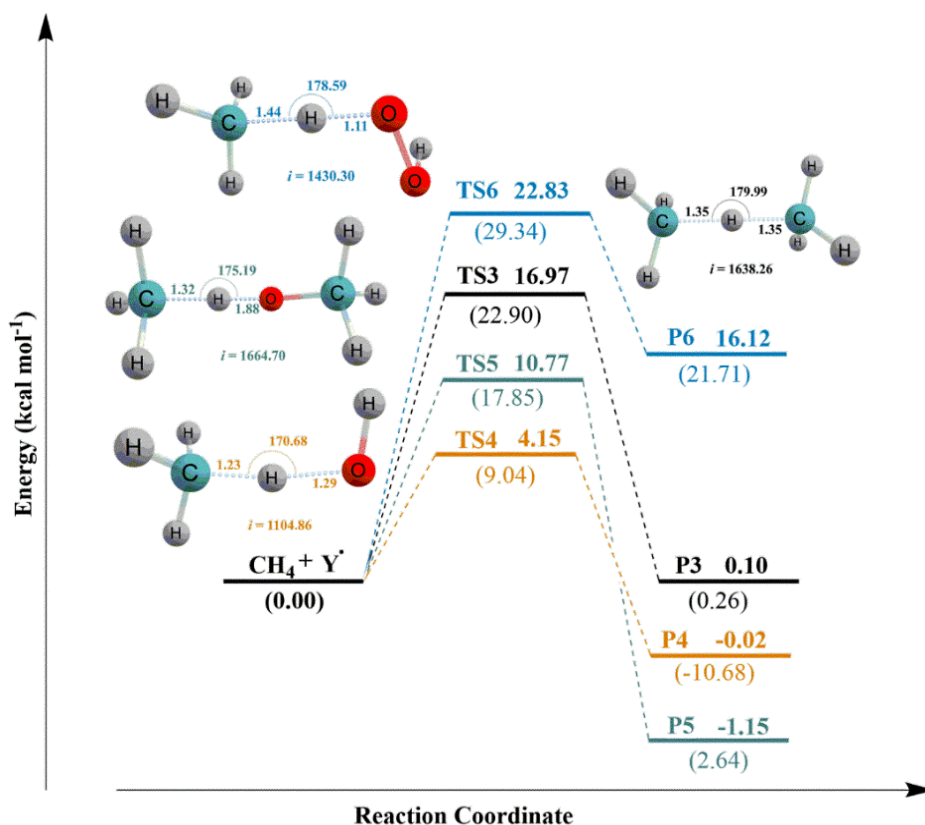


**Figure 3.2.** Optimized geometries with geometrical parameters of stationary points and qualitative representation of the potential energy profile of the reaction scheme 1.2 using CBS-QB3 theoretical method. Note that the relative electronic energy (kcal/mol) with ZP correction outside the parentheses and relative gibbs free energy with ZP correction inside the parentheses.

**Reaction between OOH radical & CH<sub>4</sub>:** Among corresponding H-abstraction barriers, TS6 possesses the highest energy barrier of 22.83 kcal/mol with an imaginary frequency of 1430.30 cm<sup>-1</sup>. Peroxide radical oxygen tends to abstract hydrogen in linear fashion from methane with the angle of 178.59° where O-H distance is 1.11 Å and C-H distance is 1.44 Å.

### Kinetics:

Other than the activation energies given in the PES, tunneling also plays significant role on the chemical rates. We are going to provide an insight into tunneling affecting the rates of chemical reactions. As mentioned earlier, tunneling is considered as a correction to the rate of reaction, taking following into account we computed the rate constant for H-abstraction reactions scheme 1.1 & 1.2 at three representative temperatures 77K, 273K, 298K shown in table 3.1, 3.2 and 3.3, respectively.

**Table 3.1.** Rate constants  $k$  ( $\text{cm}^3 \text{ molecule}^{-1} \text{ s}^{-1}$ ), quantum corrections  $\kappa$ , kinetic isotope effect ( $k_{\text{H}}/k_{\text{D}}$ ) for the H-abstraction reactions at 77K

Species	$\kappa_{\text{H}}$	$\kappa_{\text{D}}$	$k_{\text{H}}$	$k_{\text{D}}$	$k_{\text{H}}/k_{\text{D}}$
$\text{NH}_2\text{CH}_2\text{-H--CH}_3$	3.46E+19	5.01E+17	1.66E-23	6.66E-28	2.49E+04
$\text{HOCH}_2\text{-H--CH}_3$	5.79E+23	3.89E+21	1.85E-24	3.44E-29	5.38E+04
$\text{CH}_3\text{-H--CH}_3$	1.77E+31	3.39E+27	3.34E-29	2.87E-35	1.16E+06
$\text{CH}_3\text{-H--OH}$	7.65E+06	5.51E+06	4.36E-16	5.83E-19	7.48E+02
$\text{CH}_3\text{-H--OCH}_3$	7.26E+20	6.09E+18	1.00E-22	2.17E-27	4.62E+04
$\text{CH}_3\text{-H--OOH}$	4.43E+12	3.07E+12	1.30E-64	3.92E-67	3.31E+02

**Table 3.2.** Rate constants  $k$  ( $\text{cm}^3 \text{ molecule}^{-1} \text{ s}^{-1}$ ), quantum corrections  $\kappa$ , kinetic isotope effect ( $k_{\text{H}}/k_{\text{D}}$ ) for the H-abstraction reactions at 273K

Species	$\kappa_{\text{H}}$	$\kappa_{\text{D}}$	$k_{\text{H}}$	$k_{\text{D}}$	$k_{\text{H}}/k_{\text{D}}$
$\text{NH}_2\text{CH}_2\text{-H--CH}_3$	19.92	5.12	3.13E-20	1.58E-21	19.77
$\text{HOCH}_2\text{-H--CH}_3$	56.25	7.96	1.89E-21	5.34E-23	35.51
$\text{CH}_3\text{-H--CH}_3$	157.60	11.69	3.80E-24	6.56E-26	57.96
$\text{CH}_3\text{-H--OH}$	04.37	2.66	3.38E-14	3.77E-15	08.95
$\text{CH}_3\text{-H--OCH}_3$	68.13	9.62	6.13E-20	1.72E-21	35.58
$\text{CH}_3\text{-H--OOH}$	14.69	5.29	7.90E-30	6.55E-31	12.07

**Table 3.3.** Rate constants  $k$  ( $\text{cm}^3 \text{ molecule}^{-1} \text{ s}^{-1}$ ), quantum corrections  $\kappa$ , kinetic isotope effect ( $k_{\text{H}}/k_{\text{D}}$ ) for the H-abstraction reactions at 298K

Species	$\kappa_{\text{H}}$	$\kappa_{\text{D}}$	$k_{\text{H}}$	$k_{\text{D}}$	$k_{\text{H}}/k_{\text{D}}$
$\text{NH}_2\text{CH}_2\text{-H--CH}_3$	11.00	03.84	9.32E-20	7.37E-21	12.65
$\text{HOCH}_2\text{-H--CH}_3$	24.16	05.34	5.71E-21	2.89E-22	19.71
$\text{CH}_3\text{-H--CH}_3$	51.28	07.03	1.69E-23	6.18E-25	27.38
$\text{HOCH}_2\text{-H--CH}_3$	24.16	05.34	5.71E-21	2.89E-22	19.71
$\text{CH}_3\text{-H--OH}$	03.52	02.32	5.27E-14	7.46E-15	07.06
$\text{CH}_3\text{-H--OCH}_3$	30.47	06.31	1.55E-19	7.43E-21	20.88
$\text{CH}_3\text{-H--OOH}$	09.27	03.99	1.80E-28	2.05E-29	08.79

It is important to mention here that the calculated transmission coefficients,  $\kappa_{\text{H}}$ , are quite large for most of the reactions and it has huge influence on the rate. We can also calculate the contribution of tunneling on the total rate through thermal and tunneling using the following simple equation.

$$\% \text{ tunneling} = 100 \times [(k_{\text{Eckart}} - 1) / k_{\text{Eckart}}] \quad \text{--Eq.3.1}$$

where  $k_{\text{Eckart}}$  is the transmission coefficient of the Eyring equation including Eckart-tunneling within it. Eckart tunneling calculations were performed using TheRate program.<sup>28</sup> This equation Eq.3.1 demonstrates about the efficiency of tunneling. By means of computed transmission coefficient  $k$  (for H only) we illustrated that >90% of the reaction is conducted by virtue of tunneling at temperature 298K except hydroxy radical, whereas efficiency of tunnelling at  $T_{273\text{K}}$  is indicated in the table 3.4. This huge impact of tunneling pointing that “what brought this?” This can be understood by the study the of KIE analogy i.e. criteria to verify the proposed tunneling process. So, the computed studies indicated in table 3.1, 3.2 & 3.3 shows that how the KIE values changes at different temperatures, illustrating that the tunneling contribution to the rate constant is more at lower temperature.

Also, at 77K, it is alleged that >99 % of the reaction is notched up because of tunneling. For some of H-abstraction reactions of  $\text{CH}_3$  radical, experimental KIE values were reported.<sup>31</sup>

Here we are trying to authenticate our tunneling results by calculating KIEs values and comparing them with the reported experimental data. Tables 3.1, 3.2 and 3.3 collectively display the calculated KIE values at three different temperatures.

**Table 3.4.** Tunneling efficiency (%tun) calculated for the reactions of scheme 1.1 & 1.2 at temperature T = 273K & 298K

Species	% tun <sub>298</sub>	% tun <sub>273</sub>
CH <sub>3</sub> -H--CH <sub>3</sub>	98.0	99.3
NH <sub>2</sub> CH <sub>2</sub> -H--CH <sub>3</sub>	90.9	94.9
HOCH <sub>2</sub> -H--CH <sub>3</sub>	95.8	98.2
CH <sub>3</sub> -H--OH	71.6	77.1
CH <sub>3</sub> -H--OOH	89.2	93.2
CH <sub>3</sub> -H--OCH <sub>3</sub>	96.7	98.5

*Williams et. al.* in late 1980s reported an evidence of tunneling in organic reactions by computing the experimental KIE values at temperature 77K.<sup>31</sup> The reaction of methyl radical with acetonitrile and methanol shows KIE > 28,000 and >1000 respectively at the temperature of interest of 77K. However, we measured the KIE for methanol and obtained  $k_H/k_D = 53,800$  in table 3.1, this KIE is substantially larger than William's value but approachable. The difference may be due to the one-dimensional Eckart tunneling calculation which overestimates tunneling at low temperature. We also measured the KIE for methylamine and obtained  $k_H/k_D = 24,900$  in table 3.1, whereas we computed general reaction, methyl radical abstracting hydrogen from the similar substrate i.e methane and measured the KIE, found to be exceptionally larger ( $k_H/k_D = 11, 60,000$ ). It seems that the value of KIE is maximum when TS is symmetric whereas KIE decreases as the substrate changes.

We also measured KIEs for the reaction of scheme 1.2 depicting the effective approach of tunneling in table 3.1, 3.2 and 3.3. The reaction of hydroxyl radical, peroxy radical and

methoxy radical with methane shows KIE values 748, 331 and 46200 respectively at 77K. This value of KIE for hydroxyl radical and peroxy radical is evidently smaller but still contributing to reaction to be carried out through tunneling.

After the careful comparison of the PES and the tunneling corrections it is found that the symmetry and the width of the PES has a great role on tunneling. Now, let's discuss their role one by one. The reaction profile figure 3.1 studied that the reaction of methylamine with TS1 and methanol with TS2 possesses exothermicity of -8.37 kcal/mol and -11.78 kcal/mol respectively whereas methane TS3 is thermo neutral possesses negligible energy of 0.1 kcal/mol based on theoretical calculations. Consequently, the reaction of CH<sub>3</sub> radical with CH<sub>4</sub> as substrate provides symmetrical PES profile whereas the use of different substrates distorts the symmetry of the PES profile figure 3.1. Additionally, examined the reaction profile figure 3.2 which dramatizes that OH and OCH<sub>3</sub> radicals on H-abstraction from CH<sub>4</sub> exhibits the trifling exothermicity of -0.02 kcal/mol and -1.15 kcal/mol respectively whereas OOH radical on reacting with CH<sub>4</sub> is highly endothermic, 16.12 kcal/mol at 273K. The reaction profile figure 3.2 is highly asymmetric.

As noted above, tunneling probability depends upon the mass of the moving molecule, the barrier height and the barrier width. Apart from the above master outline, tunneling effect mainly depends on the shape of barrier hereby, I mean the narrowness of the PES. The imaginary vibrational frequency (IF) corresponding to the motion of molecule in transition state is major contributing factor to the narrowness of the barrier.

Thus, the IF of the all TSs are given in PES of reactions in figure 3.1 and figure 3.2. Higher the IF slimmer the barrier, resulting to the large transmission coefficient with increase in the IF of TS thus, high KIE value. This trend is followed by the TSs in the reaction scheme 1.1, where TS3 having the highest IF of 1638.26 cm<sup>-1</sup>, thus narrower the barrier and TS2 having the second highest IF of 1536.77 cm<sup>-1</sup>, wider the barrier as compared to TS3 and the TS1 having the smallest IF value of 1378.03 cm<sup>-1</sup> with widest barrier amongst three of the above shown in figure 3.1. Infrequently, this trend is untracked for the reaction scheme 1.2 due to the asymmetry nature of the PES in figure 3.2. Above mentioned postulate of IF contributing to the narrowness of the barrier can be studied with the aid of diagram like figure 3.3 showing the Eckart potential plot against the IRC of two H-abstraction reactions.

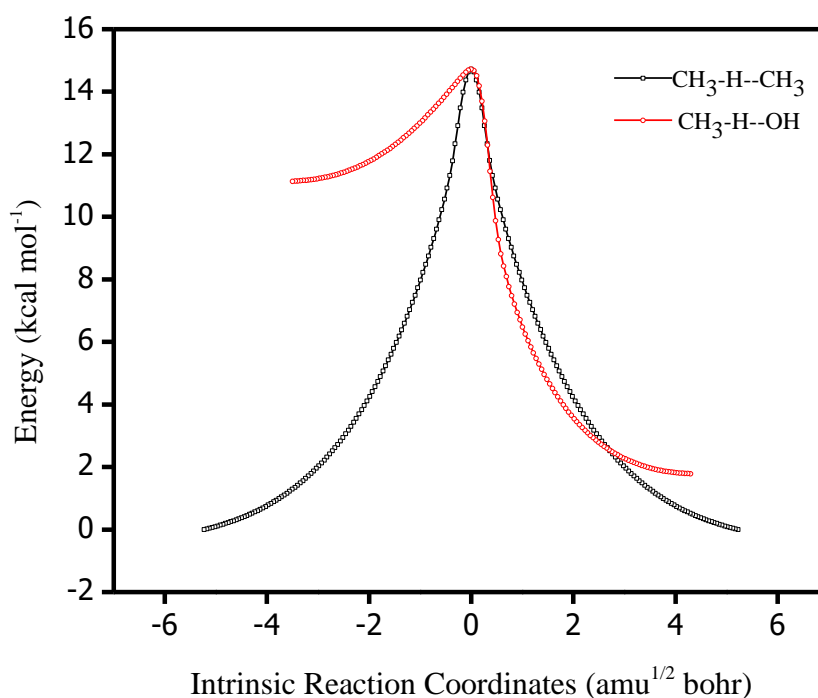


**Figure 3.3.** Potential Energy ( $E$ , kcal/mol) vs Intrinsic Reaction Coordinates ( $\text{amu}^{1/2} \text{ bohr}$ ) for H-abstraction reaction from scheme 1.2 by TS3 and TS4 computed at B3LYP/CBSB7 level of theory.

It shows that TS4 exhibits a small wide barrier in the range of -3.5 to +4.3 units of IRC in transition state region whereas TS3 possesses a sharp barrier in the range of -5.2 to +5.2 units of IRC in figure 3.3. Taking cognizance of above, the factors like height of the barrier, width of the barrier, imaginary frequency, PES symmetry or asymmetry etc. collectively controls the value of transmission coefficient i.e. the tunneling effect specifically in H-abstraction reactions. All these plausible explanations attributes to the possibility of tunneling through the potential energy barrier.

## Chapter 4

---

### Conclusion

To solve the complexity of reaction pathways and to account for the reaction rates, our study is centralized on the quantum phenomenon namely quantum mechanical tunneling. The PESs, activation energies, rate constants and transmission coefficients have been computed at high level CBS-QB3 method. QMT is found ubiquitous in hydrogen atom transfer/abstraction (HAT) reactions. We found that approximately more than 90% of the H-abstraction reactions are conducted by virtue of tunneling at temperature 298K.

This thesis also scrutinized the PESs of the systematically chosen simple H-abstraction reactions to find their role on quantum mechanical tunneling. Concluding briefly, we observed that tunneling probability is higher in case of symmetric thermoneutral PES (e.g., the reaction possesses TS3) than in the exothermic or endothermic PESs (e.g., the other reactions). The imaginary vibrational frequency contributing to the narrowness of barrier, studied using IRC calculations, also proves the higher tunneling possibility for the transformations possesses narrow barrier. Here we also authenticated our tunneling results by calculating KIE values theoretically and compared with the reported experimental data at temperature 77K, elaborately addressed in chapter 3 of this thesis. We found that our theoretically calculated KIE values deviates from reported values but are significantly approachable. Without dragging out, we led to the conclusion that mostly H-abstraction reactions exclusively follows tunneling control but at different extent and as outcome thereby tunneling is favored at lower temperature.

## References

1. Engel, T. Physical Chemistry, 3<sup>rd</sup> Edition; Pearson, 2013.
2. Bell, R. P. Tunnel Effect in Chemistry; Chapman and Hall: London, 1980.
3. Schreiner, P. R. Tunneling Control of Chemical Reactions: The Third Reactivity Paradigm. *Journal of the American Chemical Society* **139**, 15276–15283 (2017).
4. Gray, H. B. & Winkler, J. R. Electron tunneling through proteins. *Q. Rev. Biophys.* **36**, 341–372 (2003).
5. Truhlar, D. G. Tunneling in enzymatic and nonenzymatic hydrogen transfer reactions. *J. Phys. Org. Chem.* **23**, 660–676 (2010).
6. Klinman, J. P. Quantum mechanical effects in enzyme-catalysed hydrogen transfer reactions. *Trends Biochem. Sci.* **14**, 368–373 (1989).
7. Cheng, L., Doubleday, C. & Breslow, R. Evidence for tunneling in base-catalyzed isomerization of glyceraldehyde to dihydroxyacetone by hydride shift under formose conditions. *Proc. Natl. Acad. Sci.* **112**, 4218–4220 (2015).
8. Gerbig, D. & Schreiner, P. R. Formation of a Tunneling Product in the Photorearrangement of o-Nitrobenzaldehyde. *Angew. Chemie - Int. Ed.* **56**, 9445–9448 (2017).
9. Gerbig, D. & Schreiner, P. R. Hydrogen-tunneling in biologically relevant small molecules: The rotamerizations of  $\alpha$ -ketocarboxylic acids. *J. Phys. Chem. B* **119**, 693–703 (2015).
10. (a) Moss, R. A., Sauers, R. R., Sheridan, R. S., Tian, J. & Zuev, P. S. Carbon tunneling in the ring expansion of noradamantylchlorocarbene. *J. Am. Chem. Soc.* **126**, 10196–10197 (2004). (b) Gerbig, D., Ley, D. & Schreiner, P. R. Light- and heavy-atom tunneling in rearrangement reactions of cyclopropylcarbenes. *Org. Lett.* **13**, 3526–3529 (2011).
11. McMahon, R. J. Chemistry: Chemical reactions involving quantum tunneling. *Science*. **299**, 833–834 (2003).
12. Mandal, D. & Shaik, S. Interplay of Tunneling, Two-State Reactivity, and Bell-Evans-Polanyi Effects in C-H Activation by Nonheme Fe(IV)O Oxidants. *J. Am. Chem. Soc.* **138**, 2094–2097 (2016)
13. Mandal, D. *et al.* How does tunneling contribute to counterintuitive H-abstraction reactivity of nonheme Fe(IV)O oxidants with alkanes? *J. Am. Chem. Soc.* **137**, 722–733 (2015).

14. Klein, J. E. M. N. *et al.* Privileged Role of Thiolate as the Axial Ligand in Hydrogen Atom Transfer Reactions by Oxoiron(IV) Complexes in Shaping the Potential Energy Surface and Inducing Significant H-Atom Tunneling. *J. Am. Chem. Soc.* **139**, 18705–18713 (2017).
15. Lewars, E. G. *Computational Chemistry*; Springer International Publishing: Switzerland, 2016.
16. Levine, I. N. *Quantum Chemistry* (6<sup>th</sup> Edition); Pearson Prentice Hall: London, 2009.
17. David Sholl, J. A. S. *Density Functional Theory: A Practical Approach*; John Wiley & Sons, 2009.
18. Hohenberg, P. & Kohn, W. Inhomogeneous Electron Gas. *Phys. Rev.* **136**, B864–B871 (1964).
19. Kohn, W. & Sham, L. J. Self-Consistent Equations Including Exchange and Correlation Effects. *Phys. Rev.* **140**, A1133–A1138 (1965).
20. Becke, A. D. A new mixing of Hartree–Fock and local density-functional theories. **98**, 1372–1377 (1993).
21. Perdew, J. P., Burke, K. & Ernzerhof, M. Generalized Gradient Approximation Made Simple. **77**, 3865–3868 (1996).
22. Tirado-Rives, J. & Jorgensen, W. L. Performance of B3LYP density functional methods for a large set of organic molecules. *J. Chem. Theory Comput.* **4**, 297–306 (2008).
23. Montgomery, J. A., Frisch, M. J., Ochterski, J. W. & Petersson, G. A. A complete basis set model chemistry. VII. Use of the minimum population localization method. *J. Chem. Phys.* **112**, 6532–6542 (2000).
24. Montgomery, J. A., Frisch, M. J., Ochterski, J. W. & Petersson, G. A. A complete basis set model chemistry. VI. Use of density functional geometries and frequencies. *J. Chem. Phys.* **110**, 2822–2827 (1999).
25. Ochterski, J. W., Petersson, G. A. & Montgomery, J. A. A complete basis set model chemistry. V. Extensions to six or more heavy atoms. *J. Chem. Phys.* **104**, 2598–2619 (1996).
26. Chr, M. & M.S., P. Note on an Approximation Treatment for Many-Electron Systems. *Phys. Rev.* **46**, 618–622 (1934).
27. Bartlett, R. J. & Musiał, M. Coupled-cluster theory in quantum chemistry. *Rev. Mod. Phys.* **79**, 291–352 (2007).

28. Frisch, M. J.; et al. Gaussian 16, revision B.01; Gaussian, Inc.: Wallingford, CT, 2016.
29. Duncan, W. T.; Bell, R. L.; Truong, T. N. TheRate: Program for ab Initio Direct Dynamics Calculations of Thermal and Vibrational State Selected Rate Constants. *J. Comput. Chem.* **19**, 1039–1052, (1998).
30. Zhurko, G.A. and Zhurko, D.A. Chemcraft. Version 1.8 (Build 536).
31. Le Roy, R. J., Murai, H. & Williams, F. Tunneling model for hydrogen abstraction reactions in low-temperature solids. Application to reactions in alcohol glasses and acetonitrile crystals. *J. Am. Chem. Soc.* **102**, 2325–2334 (1980).

## ORIGINALITY REPORT

10%

SIMILARITY INDEX

3%

INTERNET SOURCES

6%

PUBLICATIONS

7%

STUDENT PAPERS

## PRIMARY SOURCES

- 
- |   |  |     |
|---|--|-----|
| 1 | Sanja Pudar, William A. Goddard. "Reaction Mechanism for Ammonia Activation in the Selective Ammoxidation of Propene on Bismuth Molybdates", The Journal of Physical Chemistry C, 2015<br>Publication  | 1%  |
| 2 | Debasish Mandal, Chandan Sahu, Sabyasachi Bagchi, Abhijit K. Das. "Kinetics and Mechanism of the Tropospheric Oxidation of Vinyl Acetate Initiated by OH Radical: A Theoretical Study", The Journal of Physical Chemistry A, 2013<br>Publication | 1%  |
| 3 | Submitted to Stockholms universitet<br>Student Paper   | 1%  |
| 4 | <a href="http://polen.itu.edu.tr">polen.itu.edu.tr</a><br>Internet Source  | 1%  |
| 5 | Submitted to Kenyatta University<br>Student Paper  | <1% |
| 6 | Submitted to University of Nottingham<br>Student Paper   | <1% |
-

---

7	Submitted to University College London Student Paper	<1%
8	Submitted to La Trobe University Student Paper	<1%
9	Itsaso Auzmendi-Murua, Joseph W. Bozzelli. " Thermochemical Properties and Bond Dissociation Enthalpies of 3- to 5-Member Ring Cyclic Ether Hydroperoxides, Alcohols, and Peroxy Radicals: Cyclic Ether Radical + O Reaction Thermochemistry ", The Journal of Physical Chemistry A, 2014 Publication	<1%
10	Submitted to University of Sheffield Student Paper	<1%
11	Submitted to University of Babylon Student Paper	<1%
12	Submitted to Nanyang Technological University, Singapore Student Paper	<1%
13	Submitted to Queen Mary and Westfield College Student Paper	<1%
14	Submitted to Higher Education Commission Pakistan Student Paper	<1%

---

15 Vivekananda, S.. "Characterization of ammonia phosphorus oxide  $\text{H}^3\text{NPO}^+$  ions and their neutral counterparts by mass spectrometry and computational chemistry", International Journal of Mass Spectrometry, 20010718  
Publication <1%

---

16 [edoc.ub.uni-muenchen.de](http://edoc.ub.uni-muenchen.de)  
Internet Source <1%

---

17 Submitted to University of Southampton  
Student Paper <1%

---

18 [ir.uiowa.edu](http://ir.uiowa.edu)  
Internet Source <1%

---

19 Submitted to 9561  
Student Paper <1%

---

20 Submitted to University of Central Florida  
Student Paper <1%

---

21 Jorgensen, S.. "Theoretical study of the gas phase reaction of methyl acetate with the hydroxyl radical: Structures, mechanisms, rates and temperature dependencies", Chemical Physics Letters, 20100426  
Publication <1%

---

22 Chunhui Liu, Peilin Han, Zhizhong Xie, Zhihong Xu, Donghui Wei. " Insights into  $\text{Ag}(\text{I})$ -catalyzed addition reactions of amino alcohols to

electron-deficient olefins: competing mechanisms, role of catalyst, and origin of chemoselectivity ", RSC Advances, 2018

Publication

23

Submitted to Institute of Graduate Studies,  
UiTM

Student Paper

<1%

24

Submitted to Australian National University

Student Paper

<1%

25

Cheeseman, . "Ab Initio Methods", VCD  
Spectroscopy for Organic Chemists, 2012.

Publication

<1%

26

Submitted to National University of Singapore

Student Paper

<1%

27

Submitted to University of KwaZulu-Natal

Student Paper

<1%

28

Submitted to Salisbury State University

Student Paper

<1%

29

V. I. Minkin. "Glossary of terms used in  
theoretical organic chemistry", Pure and  
Applied Chemistry, 1999

Publication

<1%

30

brage.bibsys.no

Internet Source

<1%

---

Exclude quotes      Off

Exclude matches      < 8 words

Exclude bibliography      On